Tribol Lett (2012) 48:63–75
DOI 10.1007/s11249-012-9939-2

ORIGINAL PAPER

# Thermodynamic Theory of Two Rough Surfaces Friction in the Boundary Lubrication Mode

**Iakov A. Lyashenko · Alexei V. Khomenko**

Received: 30 October 2011 / Accepted: 6 March 2012 / Published online: 5 April 2012


**Abstract** The thermodynamic theory of thin lubricant film melting, confined between two hard rough solid surfaces, is built using the Landau phase transition approach. For the description of a melting condition, the order parameter is introduced which is a periodical part of microscopic medium density function. The shear modulus of lubricant is proportional to the order parameter squared. The thermodynamic and shear melting are described consistently. A mechanical analogue of a tribological system in the boundary friction mode is studied. The time dependencies of the friction force, the relative velocity of the interacting surfaces, and the elastic component of the shear stresses appearing in the lubricant are obtained. It is shown that the shear modulus of the lubricant and the elastic stresses become zero in the liquid-like state. The irregular stick-slip mode of melting is described, which is observed in experiments. It is shown that the frequency of stiction spikes in the irregular mode increases with growth of the shear velocity. Comparison of the obtained results with experimental data is carried out.

**Keywords** Nanotribology · Boundary lubrication friction · Friction mechanisms · Stick-slip

I. A. Lyashenko (✉) · A. V. Khomenko
Peter Grunberg Institut, Forschungszentrum Jülich, 52425 Jülich, Germany
e-mail: nabla04@ukr.net

A. V. Khomenko
e-mail: khom@mss.sumdu.edu.ua

*Present Address:*
I. A. Lyashenko · A. V. Khomenko
Sumy State University, 40007 Sumy, Ukraine

## 1 Introduction

Boundary friction mode emerges if the thickness of a lubricant material between two rubbing surfaces does not exceed 10 atomic layers [1, 2]. Experiments show that thin lubricants demonstrate abnormal properties in comparison with those in the case of bulk liquids [3, 4]. In particular, the stick-slip motion mode inherent to dry friction is observed [1, 5]. Stick-slip motion is explained as a solidification induced by squeezing of rubbing surfaces, followed by an abrupt melting when shear stresses exceed the critical value ("shear melting"). There are a few phenomenological models that partially explain the results experimentally observed: thermodynamic models [6, 7], synergetic models [8, 9] etc. Methods of molecular dynamics are very often used [10–12] and give good results, however, in this case at the description of each particular experimental situation it is necessary to write down various systems of equations and it is difficult to track any general tendency. Microscopic theories often can not explain behavior of macroscopic quantities which are actually measured in real experiments [3, 4, 13]. Besides, when using computer modeling it is often impossible to describe long-term processes because of computing restrictions. The phenomenological approach, in particular shown in this study, gives the chance to bypass the specified difficulties and can help to connect the parameters of microscopic theories with macroscopic measurements.

It turns out that the lubricant can operate in a number of kinetic modes, and transitions between them take place in the course of friction, which is responsible for the stick-slip motion [3, 4]. Theoretical study in paper [14] has predicted the three modes of friction: a sliding at low shear velocities, a regular stick-slip motion, and a sliding mode at high shear velocities. Numerous experiments confirm the

existence of these modes [3, 4, 15, 16]. Thermodynamic theory proposed in study [6] is based on the expansion of the free energy of the system into a power series in the parameter $\varphi$. The $\varphi^2$ is the shear modulus of lubricant, which takes on zero value in liquid-like state of lubricant and has non-zero value in solid-like one. This approach is based on the Landau theory of phase transitions [17]. Within the framework of model developed in [6], the second-order phase transition is investigated only and in this case the stick-slip motion mode is not observed. The first- and second-order phase transitions take place in experiments [3, 4]. The first-order phase transition in ultrathin lubricant film results in the stick-slip motion [3, 4, 7]. The proposed study continues the consideration started in [7], which based on the ideas of [6]. We are aiming to study the non-regular stick-slip motion at the first-order phase transition within the framework of the models [6, 7] using a mechanical equivalent for the tribological system and taking into account the roughness of rubbing surfaces in boundary lubrication regime.

The study is devoted to description of reasons for the phenomena occurring at boundary friction. In the offered general model, the concrete types of lubricants and rubbing surfaces are not considered. Since the approach is quantitative, it can be modified to describe concrete experiments. Partly this can be done by the choice of numerical values of introduced further coefficients. Many typical boundary lubricants consist of polymer molecules bonded with polar ends to the lubricated surfaces. These situations can not be described with the presented model that is valid only for lubricants with non-polar quasispherical molecules [3, 4]. One reason for this is that in the proposed study in the liquid-like state of the lubricant, the elastic stresses are equal to zero due to the complete disordering of lubricant molecules. In the thin lubricants with polymeric molecules, the total disordering (as well as the ordering) is not always possible. Other reason is that obtained kinetic dependencies are strictly periodic that is observed only for quasispherical molecules [3, 4].

All sections of study are devoted to consideration of the lubricant with the constant thickness while in Sect. 6 generalization is carried out on rough surfaces. The detailed description of the phenomena, taking place due to spatial non-homogeneities in the lubricant, represents a separate complex problem and this is not the goal of the study. Therefore, the simplified description is resulted in Sect. 6, where the dependence of lubricant thickness on the level of surfaces non-homogeneities is taken into account. At motion of surfaces, the lubricant thickness changes everywhere that causes the variation of strain levels in plane. It is the reason for the local melting. In the case of roughness of only one surface, the stick-slip mode is regular that is also restriction and it does not occur at long polymeric molecules. It is worth noting that according to the model in the limit of small thickness of the lubricant it is liquid-like. An analogical result is obtained within the framework of approach, describing the second-order phase transition [18], where the lubricant thickness effect is discussed in detail.

## 2 Density of Free Energy

Let us introduce the density of free energy for the lubricant in the form [6, 7]:

$$f = \alpha(T - T_c)\varphi^2 + \frac{a}{2}\varphi^2\varepsilon_{el}^2 - \frac{b}{3}\varphi^3 + \frac{c}{4}\varphi^4, \tag{1}$$

where $T$ is the temperature of the lubricant, $T_c$ is the critical temperature, $\varepsilon_{el}$ is the shear component of elastic strain, $\alpha$, $a$, $b$, $c$ are the positive constants, $\varphi$ is the order parameter (the amplitude of periodical part of microscopic function of medium density [6]). Parameter $\varphi$ is equal to zero in liquid-like phase and takes on a non-zero value in solid-like structure. Such form of expansion is used for description of first-order phase transitions.

Let us define the elastic stress in the lubricant layer as $\sigma_{el} = \partial f/\partial\varepsilon_{el}$ :

$$\sigma_{el} = \mu\varepsilon_{el}, \tag{2}$$

$$\mu = a\varphi^2, \tag{3}$$

where $\mu$ is the shear modulus of lubricant. According to Eq. 1 and Eq. 3, the shear modulus $\mu$ takes on zero value when lubricant is liquid-like ($\varphi = 0$). And $\mu$ possesses a non-zero value when lubricant has solid-like structure ($\varphi > 0$).

The stationary states are defined by the condition $\partial f/\partial\varphi = 0$ [7]:

$$\varphi_{\mp} = \frac{b}{2c} \mp \sqrt{\left(\frac{b}{2c}\right)^2 - \left(\frac{a}{c}\varepsilon_{el}^2 + \frac{2\alpha(T - T_c)}{c}\right)}. \tag{4}$$

In addition to Eq. 4, the stationary state $\varphi_0 = 0$ always exists corresponding to extremum of potential given by Eq. 1 at zero value of order parameter (it may be both a maximum and a minimum of potential given by Eq. 1). According to Eq. 4, the melting of lubricant takes place when its temperature $T$ increases, as well as when the shear component of elastic strain $\varepsilon_{el}$ grows. Thus, the given model considers the thermal and shear melting, which are governed by different mechanisms.

The analysis of Eq. 4 allows us to obtain the following cases. Let us introduce the function

$$B(\varepsilon_{el}, T) = a\varepsilon_{el}^2 + 2\alpha(T - T_c). \tag{5}$$

At $B(\varepsilon_{el}, T) \le 0$, the one non-zero minimum of potential given by Eq. 1 at positive values of $\varphi$ is realized (curve 1 in Fig. 1).

In this case, the lubricant is solid-like, because the shear modulus $\mu > 0$. In the intermediate interval of values $0 < B(\varepsilon_{el}, T) < b^2/4c$ zero maximum of potential is transformed to minimum, and in addition the maximum appears separating zero minimum from non-zero one (curve 2 in Fig. 1). In such case, the lubricant can have solid-like, or liquid-like structure, depending on initial conditions. And in the case $B(\varepsilon_{el}, T) \geq b^2/4c$ single zero minimum of $f(\varphi)$ is realized (curve 3 in Fig. 1), which corresponds to zero value of shear modulus $\mu$ and liquid-like structure of the lubricant according to Eq. 3. Since the parameter $\varphi$ is the density modulation, we describe only positive values of $\varphi$, and negative values of this parameter have no physical meaning.

## 3 Phase Diagram

Let us introduce $V$ as the relative shear velocity of the rubbing surfaces divided by an ultrathin lubricant film with the thickness $h$. To find a relationship between the shear velocity and elastic strain in the lubricant film, we will use the Debye approximation relating the elastic strain $\varepsilon_{el}$ and the plastic one $\varepsilon_{pl}$ [6]:

$$\dot{\varepsilon}_{pl} = \frac{\varepsilon_{el}}{\tau_\varepsilon}, \tag{6}$$

where $\tau_\varepsilon$ is the Maxwell relaxation time for internal stress. The total strain in the lubricant is defined as the sum of elastic and plastic components:

$$\varepsilon = \varepsilon_{el} + \varepsilon_{pl}, \tag{7}$$

and it fixes the motion velocity of the top block $V$ according to the well-known relationship [19]:

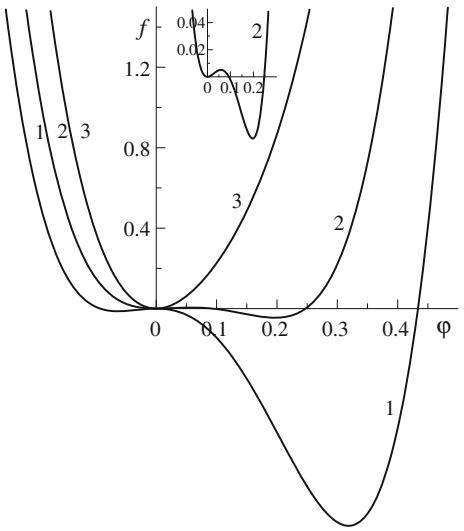


**Fig. 1** Dependence of density of free energy $f$ (J/m$^3$) given by Eq. 1 on order parameter $\varphi$ (dimensionless variable) at $\alpha = 0.95$ J K$^{-1}$/m$^3$, $T_c = 290$ K, $a = 2 \cdot 10^{12}$Pa, $b = 230$ J/m$^3$, $c = 900$ J/m$^3$. *Curves* 1–3 correspond to the temperatures $T = 271$, 286, 310(K) and $\varepsilon_{el} = 3 \cdot 10^{-6}$

$$V = h\dot{\varepsilon} = h(\dot{\varepsilon}_{el} + \dot{\varepsilon}_{pl}). \tag{8}$$

The last three equalities give the expression for the elastic component of shear strain [7]:

$$\tau_\varepsilon \dot{\varepsilon}_{el} = -\varepsilon_{el} + \frac{V\tau_\varepsilon}{h}. \tag{9}$$

At constant shear velocity $V$, the stationary value of elastic strain is defined by Eq. 9:

$$\varepsilon_{el}^0 = \frac{V\tau_\varepsilon}{h}. \tag{10}$$

In the general case, free energy given by Eq. 1 depends on the thickness of lubricant $h$ [18]. It is worth noting that the second term in Eq. 1 depends on the square of elastic strain $\varepsilon_{el}^2$. According to Eq. 10, the stationary elastic strain increases with thickness $h$ decreasing. Therefore in the limit $h \to 0$ of very thin lubricant the strain $\varepsilon_{el} \to \infty$. Thus, in expansion given by Eq. 1 the second term is determining, and the stationary value of the order parameter is equal to zero, consequently the lubricant is liquid-like similar to the study [18]. Study of the lubricant thickness effect has been carried out in Refs. [20, 21] also.

According to the principle of minimum of energy, the system tends to occupy a state corresponding to the minimum of potential $f(\varphi)$ at any initial conditions (see Fig. 1). Thus, the stationary value of the order parameter sets in, defined by the Eq. 4, where the sign "+" meets the stable state (the minimum) and the sign "−" corresponds to unstable one (the maximum). In Fig. 2, the stationary values of order parameter are shown, which are calculated according to Eq. 4, in which the stationary elastic strain $\varepsilon_{el}$ is defined by the Eq. 10. The solid parts of curves correspond to the stable stationary states, and the dashed lines meet the unstable ones.

At zero shear velocity (the shear stress and strain are equal to zero) and small value of the temperature $T$, the lubricant is solid-like, because a non-zero value of order parameter $\varphi$ is realized, and according to Eq. 3 the shear modulus $\mu$ is not equal to zero either (Fig. 2a, solid section of curve 1). In this case, the potential is shown by curve 1 in Fig. 1. If the temperature $T$ exceeds the critical value

$$T_{c0} = T_c - \frac{a}{2\alpha}\left(\frac{\tau_\varepsilon V}{h}\right)^2 + \frac{b^2}{8\alpha c} \tag{11}$$

the order parameter $\varphi$ changes abruptly from non-zero value

$$\varphi_A = \frac{b}{2c} \tag{12}$$

to zero with transition of the lubricant in liquid-like state, and curve 3 in Fig. 1 depicts this. If after this transition, the value of $T$ decreases, the lubricant solidifies at lower temperature:

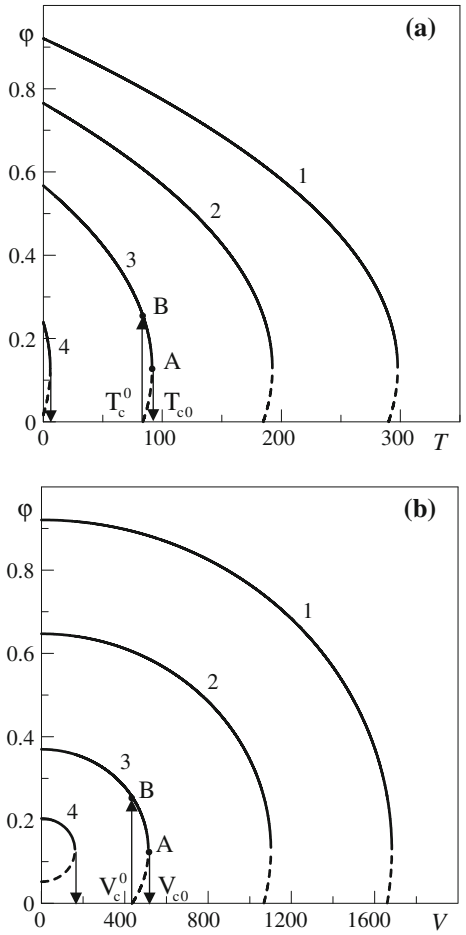


**Fig. 2** Dependence of stationary value of order parameter $\varphi$ given by Eq. 4 on temperature of lubricant $T$ (K) and shear velocity $V$ (nm/s) at parameters of Fig. 1 and $h = 1$ nm, $\tau_\varepsilon = 10^{-8}$ s. **a** *Curves* 1–4 correspond to the fixed values of shear velocity $V = 0$, 900, 1400, 1665 (nm/s); **b** *curves* 1–4 correspond to the fixed temperatures $T = 0$, 170, 270, 295 (K). In this figure and in further ones, the transitions are shown by *arrows* not for all curves for better recognition of figures

$$T_c^0 = T_c - \frac{a}{2\alpha}\left(\frac{\tau_\varepsilon V}{h}\right)^2. \tag{13}$$

Thus, the abrupt change of the order parameter from zero to non-zero value

$$\varphi_B = \frac{b}{c} \tag{14}$$

is observed.

The potential in the intermediate interval $T_c^0 < T < T_{c0}$ is shown by curve 2 in Fig. 1. Therefore, the dependence $\varphi(T)$ has hysteresis character and corresponds to the first-order phase transitions. The reasons for hysteresis behavior have been discussed earlier within the framework of synergetic model in the paper [22]. According to Fig. 2a, the lubricant melts at smaller value of the temperature with increase in the shear velocity. Curve 4 corresponds to the case when the lubricant can not solidify after melting with decrease in the temperature. If the velocity is higher than a certain critical value, the lubricant is liquid-like ($\mu = 0$) at any temperature.

According to Fig. 2b, when the velocity exceeds the critical value

$$V_{c0} = \frac{h}{\tau_\varepsilon}\sqrt{\frac{2\alpha(T_c - T)}{a} + \frac{b^2}{4ac}} \tag{15}$$

the melting of lubricant occurs, and if $V$ is less than the value

$$V_c^0 = \frac{h}{\tau_\varepsilon}\sqrt{\frac{2\alpha(T_c - T)}{a}} \tag{16}$$

the lubricant solidifies. Here, the situation is similar to the one presented in Fig. 2a.

But some different features exist in these figures. In Fig. 2a, the width of the hysteresis loop is constant at all velocities $V$. The width of the hysteresis loop $\Delta T$ can be obtained from Eqs. 11 and 13:

$$\Delta T = T_{c0} - T_c^0 = \frac{b^2}{8\alpha c}. \tag{17}$$

According to Eqs. 15 and 16, the width of the hysteresis loop $\Delta V$ in Fig. 2b increases with growth of the temperature. Similar result was obtained within the framework of other model [23, 24]. Velocity and temperature differently influence on the width of hysteresis $\Delta T$ and $\Delta V$ because the temperature $T$ is included in the first power in potential given by Eq. 1, and the shear elastic strain $\varepsilon_{el}$ has the second power and is connected with the velocity of motion $V$ by the linear relationship 10.

In Fig. 3, the dependencies of critical velocity of lubricant melting $V_{c0}$ given by Eq. 15 and of its solidifying $V_c^0$ given by Eq. 16 on the temperature $T$ are shown. Above the curve $V_{c0}$, the lubricant is liquid-like and the sliding friction regime (SF) is realized. In the interval $V < V_c^0$, the lubricant has solid-like structure. Between curves in Fig. 3, the potential $f(\varphi)$ looks like the curve 2 in Fig. 1, therefore the lubricant state in this area depends on initial conditions. Thus, Fig. 3 represents the phase diagram with two stationary friction modes. Figure 3 can be interpreted also as the dependence of critical temperatures $T_{c0}$ given by Eq. 11 and $T_c^0$ given by Eq. 13 on the shear velocity $V$. It is worth noting that between curves in the diagram there is the domain of the above mentioned hysteresis which always takes place at the first-order phase transitions. Stick-slip friction mode examined further, which is often observed in such systems experimentally [1–4], is the consequence of the first-order phase transition [25]. However, it is not worth considering that exactly in this area of diagram the stick-slip mode of friction

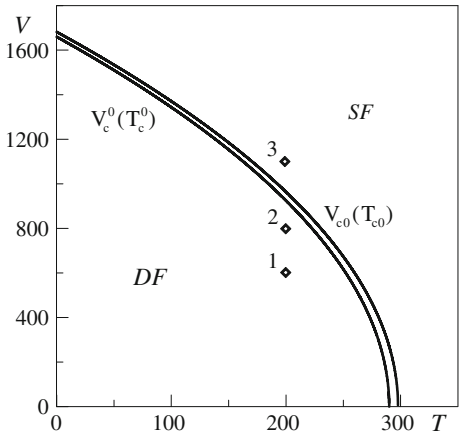


**Fig. 3** Phase diagram with domains of liquid-like (SF) and solid-like (DF) lubricant at parameters of Fig. 2

is realized in the real experiment. For examined further tribological system, which is the analogue of experimental situation, for the parameters of point 1 in the phase diagram the stationary mode of dry friction is realized that is characterized by constant non-zero value of elastic stresses $\sigma_{el}$ (see Fig. 6). While for the parameters of point 2, which as well as point 1 in Fig. 3 is in the area of dry friction, the stick-slip motion is observed (see Fig. 7). It takes place owing to that the friction mode is determined by the whole tribological system parameters, e.g., lubricant viscosity, mass of the rubbing block, spring rigidity (see Fig. 5). Therefore, velocity $V$, shown in the axis of Fig. 3, is not definitely determined by spring velocity $V_0$ in Fig. 5 that leads to the stick-slip mode. If an overhead block is moved not by spring, but with the fixed velocity $V$ (replacing spring by the rigid coupling), the phase diagram in Fig. 3 is observed. However, in domain of hysteresis, depending on the initial state of the lubricant (DF or SF), the dry friction DF or the sliding SF is realized at motion, but not stick-slip mode. This is standard situation for the first-order phase transitions. Dynamic phase diagram of the lubricant states for the system depicted in Fig. 5 has complicated form substantially dependent on the parameters of concrete experimental system. The construction of this diagram represents more complex problem, that is not the purpose of the offered study. Such phase diagrams are obtained both experimentally [1, 3, 4] and theoretically [21].

## 4 Friction Map

At shear of rubbing surfaces in the layer of lubricant elastic stress $\sigma_{el}$ and viscous stress $\sigma_v$ appear. The total stress is the sum of these components:

$$\sigma = \sigma_{el} + \sigma_v. \tag{18}$$

The friction force $F$, which interferes with the movement, can be found as a product of total stress $\sigma$ and area of rubbing surfaces $A$:

$$F = \sigma A. \tag{19}$$

Let us define the viscous stress in the lubricant layer according to the formula [19]

$$\sigma_v = \frac{\eta_{eff} V}{h}, \tag{20}$$

where $\eta_{eff}$ is the effective viscosity of lubricant material. It is worth noting that according to Eq. 20, the viscous stresses are in both liquid-like and solid-like lubricant states. The presence of the viscous (dissipative) stresses in both phases was shown in experimental study [26]. However, in the solid-like lubricant state, the viscous stresses take on small values since in accordance with Eq. 20 they are proportional to the shear velocity $V$ that is small in the solid-like state. The boundary lubricant is the non-Newtonian liquid. Such lubricants have complex $\eta_{eff}(\dot{\varepsilon})$ dependencies. For example, viscosity of pseudoplastic lubricants decreases with increasing in shear rate $\dot{\varepsilon}$, and for dilatant lubricants the viscosity increases with growth of $\dot{\varepsilon}$. Therefore, we use the simple approximation [19]

$$\eta_{eff} = k(\dot{\varepsilon})^{\gamma}, \tag{21}$$

allowing us to consider both cases qualitatively. Here, the proportionality factor $k(\mathrm{Pa\,s}^{\gamma+1})$ is introduced.

With the account of Eqs. 8 and 21, the expression for the viscous stresses given by Eq. 20 takes on the form:

$$\sigma_v = k\left(\frac{V}{h}\right)^{\gamma+1}. \tag{22}$$

Having substituted Eqs. 18 and 22 into Eq. 19, we obtain the final equation for friction force [7]:

$$F = \left[\sigma_{el} + k \cdot \mathrm{sgn}(V)\left(\frac{|V|}{h}\right)^{\gamma+1}\right] A, \tag{23}$$

where the elastic stress $\sigma_{el}$ is defined by Eq. 2.

The dependence given by Eq. 23 is shown in Fig. 4.

Figure 4a shows that the friction force decreases at the fixed shear velocity with increase in the temperature. It occurs because of the decrease in the shear modulus. When lubricant melts ($T > T_{c0}$), the friction force does not depend on the temperature, since within the considered model the shear modulus is equal to zero in this case. The dependencies are characterized by hysteresis, because at phase transition the shear modulus given by Eq. 3 changes abruptly.

Figure 4b shows a different behavior. Here, according to Eq. 23, at increase in velocity the total friction force at first

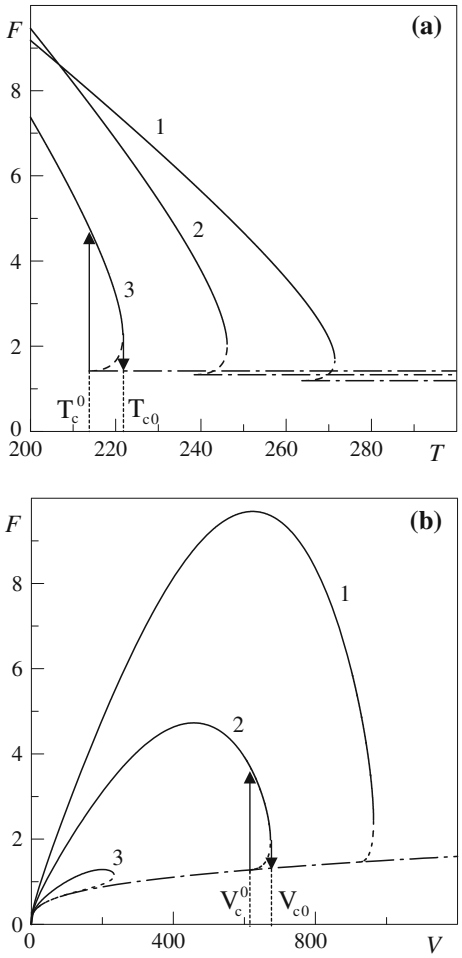


**Fig. 4** Dependence of friction force $F$ (mN) given by Eq. 23 on temperature $T$ (K) and shear velocity $V$ (nm/s) at parameters of Fig. 2 and $\gamma = -2/3$, $A = 3 \cdot 10^{-9}\text{m}^2$, $k = 5 \cdot 10^4$ Pa $\text{s}^{1/3}$. **a** *Curves* 1–3 correspond to the constant values of shear velocity $V = 500, 700, 850$ (nm/s); **b** *curves* 1–3 correspond to the fixed values of temperature $T = 200, 250, 292$ (K)

grows due to the increase in the viscous stresses $\sigma_v$, and because of the increase in the elastic component of $F$ caused by the increase in the elastic component of strain given by Eq. 10. However, the shear modulus decreases with growth of velocity leading to reduction of the elastic component of force $F$. Therefore, a critical velocity exists above which the lubricant still remains solid-like, however, the total friction force starts to decrease. With further increase in the velocity at $V > V_{c0}$ given by Eq. 15 the melting occurs, and the elastic stress given by Eq. 2 becomes equal to zero. Therefore, the first term in Eq. 23 is equal to zero also and that leads to abrupt decrease in total friction force. If $V$ increases furthermore, the value $F$ increases due to the viscous component (the second term in Eq. 23). The lubricant solidifies at abrupt increase in force $F$ but at a different value of velocity $V = V_c^0$ given by Eq. 16. Let us note that in Fig. 4b, the dependencies of friction force after melting coincide for all curves, since the viscous component of $F$ depends on the shear velocity only and does not depend on the temperature. In Fig. 4b, curve 3 differs from others, because its solid part (stable value of $F$ before melting) and dashed part (unstable value of $F$) together make a closed line. In addition, the friction force after melting is always described by the dependence shown in figure by dash-dotted line (stable value of $F$ after melting), since the lubricant can not solidify with decrease in $V$ anymore.

Actually Fig. 4 represents a friction map for boundary lubrication regime. This figure shows the lubricant state (solid-like lubricant with big friction force or liquid-like lubricant with small value of friction force) depending on system parameters.

## 5 Kinetic Regimes

The dynamic characteristics of real tribological systems are defined by the properties of system as a whole. In particular, in the hysteresis region of the dependence in Fig. 3, the stick-slip mode of friction can be realized. A typical scheme of tribological system is presented in Fig. 5. Here, the spring of rigidity $K$ is connected to the block of mass $M$. The block is located on a smooth surface from which it is separated by the layer of lubricant with thickness $h$. The free end of the spring is brought in motion with a constant velocity $V_0$. Block motion initiates friction force $F$ given by Eq. 23 that resists its displacement. Generally, in a boundary friction mode, the velocities of block $V$ and spring $V_0$ do not coincide because of the oscillating character of force $F$ leading to stick-slip motion of the block.

Let us introduce $X$ as the coordinate of the top block. According to this, the equation of motion looks like [3, 4, 6, 7]

$$M\ddot{X} = K\Delta X - F. \tag{24}$$

Here, $\Delta X$ is the spring tension, which can be defined as

$$\Delta X = \int_0^t V_0 \mathrm{d}t' - X, \tag{25}$$

where $t = t'$ is the motion time of free end of the spring. In the case when the value of $V_0$ does not vary during time Eq. 25 has the form

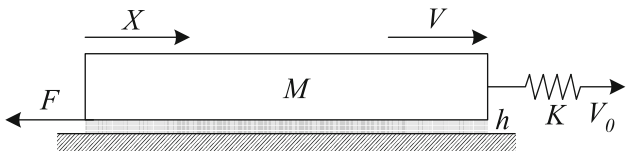


**Fig. 5** The scheme of tribological system

$$\Delta X = V_0 t - X. \tag{26}$$

The abrupt change of the lubricant temperature and strain leads to variation of order parameter, over which value $\varphi$ the free energy $f$ is developed in the power expansion given by Eq. 1 [17]. The time to rich the new stable stationary value $\varphi_+$ given by Eq. 4 is determined by the generalized thermodynamic force $-\partial f/\partial\varphi$. If $\varphi \approx \varphi_+$ this force is small and relaxation process of transition to equilibrium is described by the linear kinetic equation [27][1]:

$$\dot{\varphi} = -\delta \frac{\partial f}{\partial \varphi}, \tag{27}$$

where $\delta$ is the kinetic coefficient characterizing the inertial properties of the system. After substitution of energy given by Eq. 1 in Eq. 27, we obtain the equation in the explicit form:

$$\dot{\varphi} = -\delta\left(2\alpha(T - T_c)\varphi + a\varphi\varepsilon_{el}^2 - b\varphi^2 + c\varphi^3\right). \tag{28}$$

To calculate the time evolution of the system the last equation is to be solved together with Eqs. 24 and 9. At calculation, we must use the relation $\dot{X} = V$. However, the relaxation time of strain $\tau_\varepsilon$ is small. Therefore, the two Eqs. 24 and 28 are solved jointly and the strain is defined from Eq. 10.

The result of calculation is shown in Fig. 6. This figure depicts the time dependencies of friction force $F(t)$, shear velocity of top block $V(t)$, coordinate of this block $X(t)$, spring tension $\Delta X(t)$, and elastic shear stresses $\sigma_{el}(t)$ appearing in the lubricant. All dependencies are built at the parameters, which correspond to the point 1 in the phase diagram, shown in Fig. 3. Thus, dependencies meet the parameters of dry friction regime DF. Figures 6, 7, and 8 are separated in two parts: if $t < 6$ s, the shear velocity $V_0$ has non-zero value, but when $t > 6$ s, the driving device is stopped, and $V_0 = 0$. Figure 6 shows that stationary regime of dry friction sets in during time if $V_0 = 600$ nm/s. In this mode, the top rubbing block shifts with the constant velocity $V$, which coincides with velocity of motion of the spring's free end $V_0 = 600$ nm/s. This occurs because in this particular case in the stationary regime the tension of spring $\Delta X$ remains constant, that is equivalent of inflexible connection of the top rubbing surface with the driving device. Since the velocity $V$ is not variable and the lubricant is solid-like with constant elastic stress $\sigma_{el}$, the friction force $F$ also does not change with time. The coordinate $X$ increases with time, because the system is in motion. After time $t > 6$ s, the velocity of free end of spring is equal to zero, all parameters

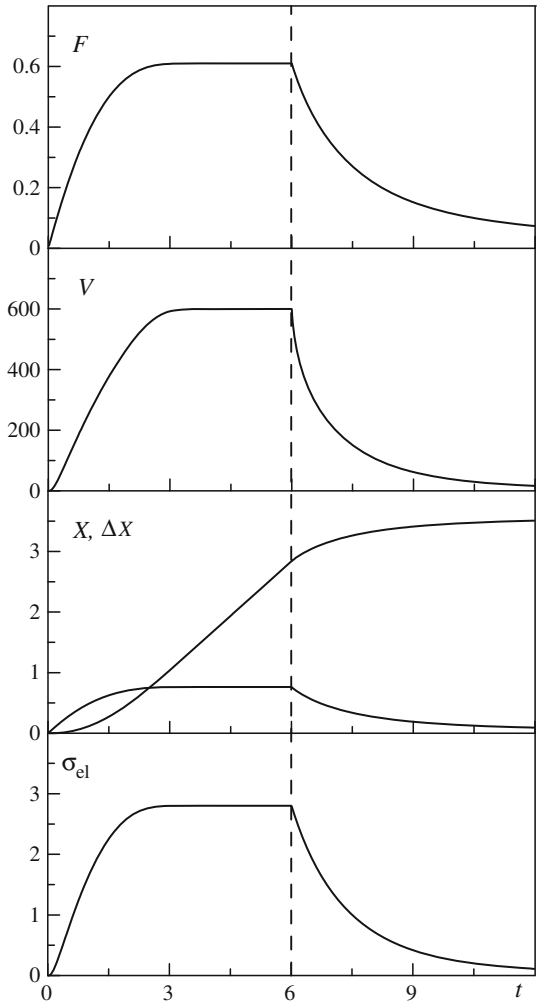


**Fig. 6** Dependencies of friction force $F$ (mN), shear velocity $V$ (nm/s), coordinate of top block $X$ (μm), spring tension $\Delta X$(μm), elastic shear stress $\sigma_{el}$ (MPa) on time $t$ (s) at parameters of Fig. 1 and $A = 0.15 \cdot 10^{-9}\,\mathrm{m}^2$, $\gamma = -2/3$, $k = 1.5 \cdot 10^5 \mathrm{Pa\,s}^{1/3}$, $M = 0.5\,\mathrm{kg}$, $K = 800\,\mathrm{N/m}$, $\delta = 100\,\mathrm{J}^{-1}\ \mathrm{m}^3/\mathrm{s}$, $T = 200\,\mathrm{K}$. Before *dashed vertical line* $V_0 = 600$ nm/s, and after this line $V_0 = 0$ nm/s

relax to zero values, and coordinate $X$ relaxes to constant non-zero value. It takes place because $\Delta X$ decreases during time and elastic force $K\Delta X$ reduces too. The main reason for such behavior is that the friction force $F$ does not have static components in this model [29]. And at zero velocity $V = 0$, friction force $F$ always has zero value.

In Fig. 7, the similar dependencies are shown for point 2 in phase diagram that is also within the dry friction area.

However, as we can see, the stick-slip friction mode sets in here, which is characterized by saw-like form of the $F(t)$ dependence. The reason for this is that the properties of the tribological system, shown in Fig. 5, are determined by the properties of the whole system, and the phase diagram depicted in Fig. 3 is built at constant shear velocity $V$. In the dynamic case, when the velocity $V_0$ is constant, the

[1] Equation 27 was introduced by Landau and Khalatnikov [28] to study the anomalous ultrasound absorption in the vicinity of phase transition.

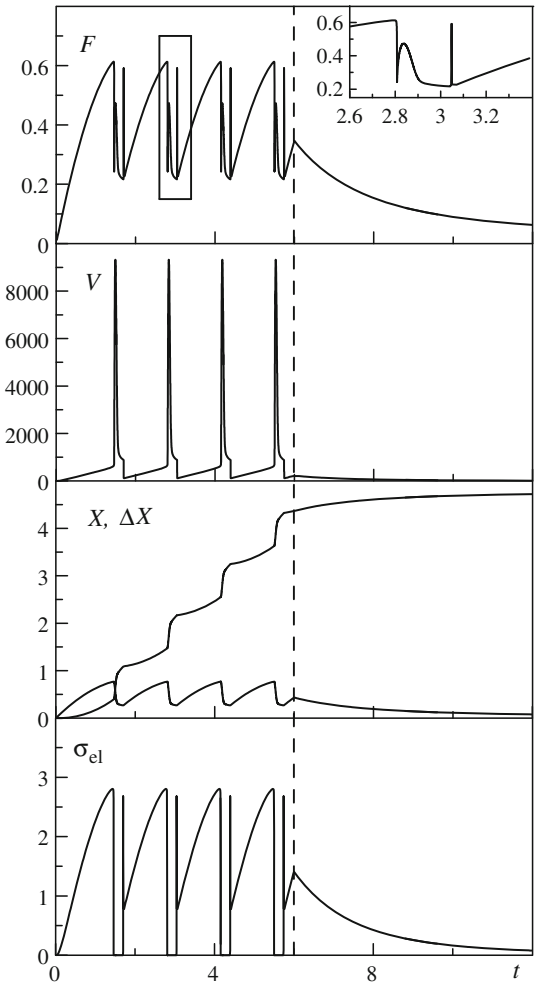


**Fig. 7** The kinetic dependencies of system quantities at parameters of Fig. 6. Before *dashed vertical line* $V_0 = 800$ nm/s, and after this line $V_0 = 0$ nm/s

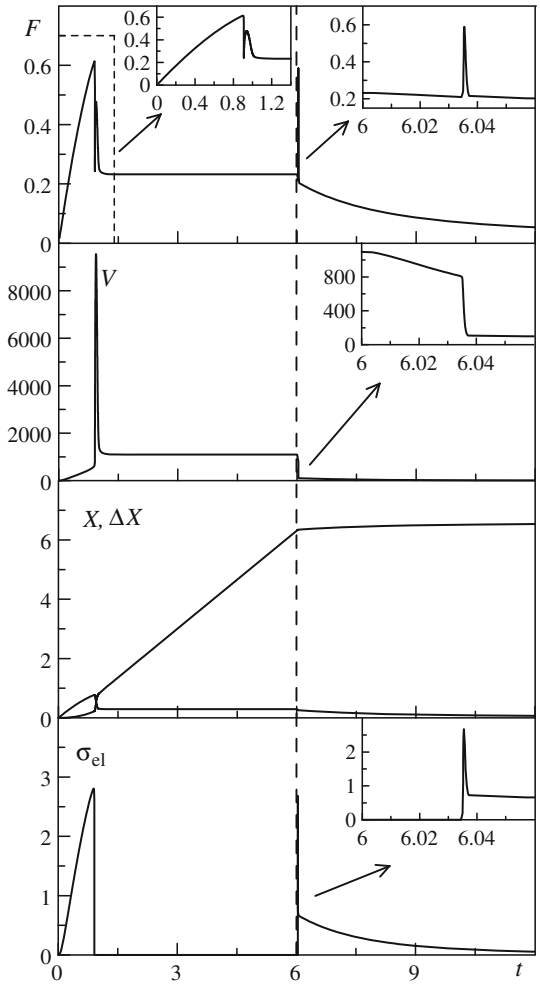


**Fig. 8** The kinetic dependencies of system quantities at parameters of Fig. 6. Before *dashed vertical line* $V_0 = 1100$ nm/s, and after this line $V_0 = 0$ nm/s

velocity $V$ strongly depends on the spring rigidity $K$ and on the coefficient $k$, which determines the contribution of the viscosity in the total friction force given by Eq. 23 and so on. Therefore, for tribological system the phase diagram has more complex form that requires more detailed study. Let us consider Fig. 7 in more details. At the moment of time $t = 0$ the movement begins, the spring tension $\Delta X$ is increased that leads to the growth of elastic force $K\Delta X$ due to the enhancement of increase in the elastic stress $\sigma_{el}$ and friction force $F$. The velocity of movement of the upper rubbing block $V$ is also increasing. When the velocity $V$ exceeds the critical value given by Eq. 15, the lubricant melts and the elastic stress is equal to zero. Accordingly, the friction force decreases sharply, since the movement velocity of the block $V$ increases sharply, and it slips on a significant distance during a short period of time. Due to such sharp slip the spring tension $\Delta X$ decreases, that leads to reduction of the shear velocity $V$, and when it becomes less than the value given by Eq. 16 the lubricant solidifies. The described process is periodic in time. For the dependence $F(t)$ in the inset after melting and a sharp decrease in friction force the two maxima are observed. The first maximum corresponds to the liquid-like lubricant, when the friction force possesses large value due to the increase in the viscous components of stress given by Eq. 22 at big shear velocity $V$. The second narrow peak meets the solidification of the lubricant and a sharp appearance of elastic stress in it. This maximum is very narrow due to sharp decrease in the shear velocity $V$ after solidification of the lubricant leading to reduction of the full friction force $F$ given by Eq. 23. After decreasing, the force $F$ grows again until the subsequent melting of the lubricant. Let us note that within the framework of proposed model at stick-slip motion, the narrow peak is always present when lubricant solidifies (see inset in the top panel in Fig. 7). However, the peak height strongly depends on the lubricant viscosity and parameters

of tribological system shown in Fig. 5. It may be lower but we have chosen parameters at which it is well expressed in dependencies. We do not know experimental studies with the presence of such peak, therefore it is prognostication. Due to high rate of relaxation of elastic stresses $\sigma_{el}$, the peak is very narrow. Its width in our study is about 0.002 s. The interval of measuring must be yet less than above mentioned for synonymous exposure of such peak in experiment. Experiments are unknown for us, where measuring is carried out so often. In more detail, the section with the peak of dependence of friction force on time is described in recently published study [30] using more simple symmetric expansion. This peak arises when lubricant solidifies similar to the "stopping spike" which is obtained in experiment [31]. The "stopping spike" is realized in proposed study in Fig. 8 after stopping of driving spring at $t > 6$ s. Also the narrow peak of friction force was observed after melting within the framework of approach offered in Ref. [21].

Dependencies, shown in Fig. 8, were built for the parameters of the point 3 in the phase diagram, which is in the area of sliding friction SF.

At this temperature $T$, according to the phase diagram in the state of rest $V = 0$, the lubricant is solid-like. So, in Fig. 8 at the beginning of the movement, all parameters monotonically increase. At the condition of melting given by Eq. 15, the lubricant melts, and elastic stress $\sigma_{el}$ relaxes to zero value that leads to the reduction of the friction force, to a sharp increase in the shear velocity $V$, and a rapid sliding of the rubbing surface on a significant distance. At the same time the spring tension $\Delta X$ is reduced. In the dependence $F(t)$, as in Fig. 7, after melting the maximum of viscous friction force is realized. However, the subsequent peak of solidification for $t < 6$ s is not observed, because at the parameters of figure the shear velocity $V$, setting in after melting, is always larger than the value given by Eq. 16 at which lubricant solidifies. Thus, in the case under consideration the kinetic regime of liquid friction is realized in the system. In this mode, the lubricant is liquid-like that provides the minimal resistance to the movement by the friction force $F$. Note that in this regime, the stationary shear velocity $V$ coincides with the value $V_0$ similar to the case shown in Fig. 6. After time $t > 6$ s, the solidification of lubricant and further relaxation of main parameters is observed.

In Fig. 9, the dependence $F(t)$ at the increase in shear velocity $V_0$ is shown. For parameters of the top panel at velocity of first part of the figure, the lubricant has solid-like structure and dry friction mode is realized. In the second part, the stick-slip mode is realized with increase in velocity. It is visible that with further increase in velocity (third part) the frequency of stick-slip transitions is larger. And at value $V_0 = V_{04}$ the lubricant has liquid-like structure. At higher temperature (the bottom panel of Fig. 9),

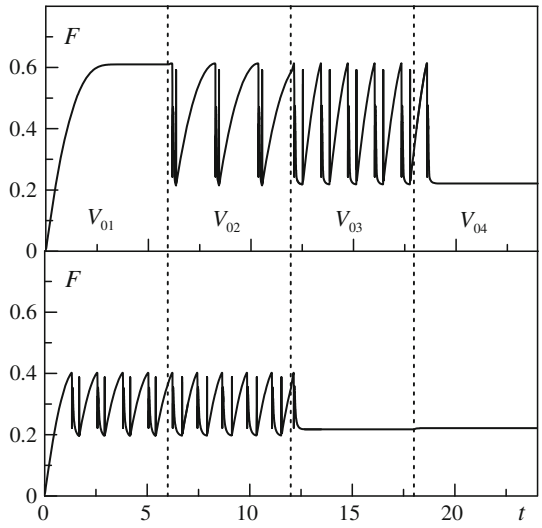


**Fig. 9** The kinetic dependencies of friction force $F$ (mN) at parameters of Fig. 6 and velocities $V_{01} = 600$, $V_{02} = 650$, $V_{03} = 900$, $V_{04} = 950$ (nm/s). The *top panel* in the figure corresponds to the temperature $T = 200$ K, and the *bottom panel* meets the value $T = 240$ K

the friction force decreases and melting of the lubricant is observed at lower velocities.

In Fig. 10, the dependence of friction force $F(t)$ at the increase in the temperature is shown. In top panel at the temperatures of first two parts, the lubricant is solid-like and the stationary value of friction force is constant. But for the second part the value of $F$ is less because the temperature is higher. In the third part, the stick-slip motion is realized, since at this temperature the lubricant already can melt. And in the last part, the lubricant melts fully, and the kinetic regime of sliding occurs. The bottom panel of Fig. 10 is build at higher value of velocity $V_0$. As we can see, in this case the lubricant melts at smaller temperatures. For parameters of bottom panel, the lubricant is not observed in solid-like steady state.

## 6 Simple Model for Rough Surfaces

In previous sections, we considered the case when the friction surfaces have atomically flat structure. This situation is possible for small domain of contact area. In real friction mechanisms, the surfaces are always rough. Let us use the Ornstein-Uhlenbeck process $\lambda(t)$ [32] for generation of the surfaces with random roughness. For numerical realization of $\lambda(t)$, the following iterative procedure is used [33]:

$$\lambda_{n+1} = \lambda_n \left(1 - \frac{\Delta t}{\tau_\lambda}\right) - \frac{\sqrt{\Delta t}}{\tau_\lambda} W_n, \tag{29}$$

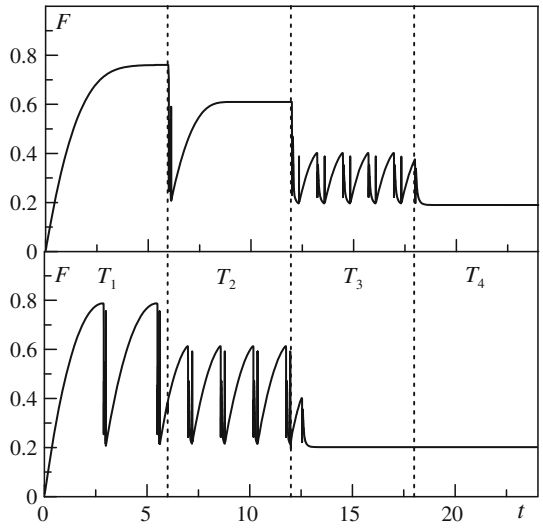


**Fig. 10** The kinetic dependencies of friction force $F$ (mN) at parameters of Fig. 6 and the temperatures $T_1 = 170$, $T_2 = 200$, $T_3 = 240$, $T_4 = 280$ (K). The *top panel* in the figure corresponds to the velocity $V_0 = 600$ nm/s, and the *bottom panel* meets the value $V_0 = 720$ nm/s

where $\tau_\lambda$ is the correlation time, $W_n$ is the random force [34]:

$$W_n = \sqrt{2I}\sqrt{-2\ln r_1}\cos(2\pi r_2), \quad r_i \in (0,1]. \tag{30}$$

Here $2I$ is the dispersion, $r_1$ and $r_2$ are the pseudo-random numbers with uniform distribution.

Let us consider the system shown in Fig. 11. In this figure, we have the top rough block which is separated from lower rough surface by the lubricant layer. At first consider the simplest 2D model with roughness in single $X$ direction. We assume that distance between all points of top and bottom surfaces is not changed in direction which is perpendicular to motion. The minimal distance between surfaces $l$ is shown by dashed lines in the figure. At further calculations, the constant value of the distance is $l = 1$ nm. For all kinetic dependencies in previous sections, we used the value of contact area $A = 0.15 \cdot 10^{-9}\text{m}^2$. If the top block has the square form, the length of this block is equal to $L = \sqrt{A} = \sqrt{0.15 \cdot 10^{-9}} \approx 0.12 \cdot 10^{-4}$ m. The procedure of obtaining the time dependencies for the case shown in Fig. 11 is analogue to previous way. The main difference is that the distance between surfaces $h$ is not constant. At solving the equations of motion, we separate the contact area of surfaces by $N$ segments. After that $h_i, \varepsilon_{\text{el},i}, \varphi_i, \sigma_{\text{el},i}, F_i$ are calculated for all segments separately. The friction force for each segment is defined by

$$F_i = \left[\sigma_{\text{el},i} + k\ \text{sgn}(V)\left(\frac{|V|}{h_i}\right)^{\gamma+1}\right]\frac{L^2}{N}, \tag{31}$$

where $L^2$ is the total contact area and $N$ is the number of segments. After that the full friction force is calculated as $F = \sum F_i$ and with this value we solve the kinetic Eq. 24. Further, the new values of $X, V, \Delta X$ are obtained and the procedure is repeated again. Since the coordinate $X$ of the top block increases during process of motion, according to Fig. 11, we obtain $h_i$ in different moments of time, and time dependencies of main quantities ($F(t)$, $V(t)$, etc.) have stochastic components [35].

Figure 12 shows the time dependencies of total friction force $F$ and shear velocity $V$ of the top rubbing block as a result of friction process modeling for rough surfaces, which is depicted in Fig. 11.

In this figure, it is visible that the both quantities are changed during time, and velocity $V$ has a stochastic component [35, 36]. But in [35, 36] in order to take into account random effects the stochastic terms were introduced into the basic equations. In this study, the stochastic behavior is the result of roughness of rubbing surfaces. Figure 12 shows that the system has the properties of dry friction regime because the friction force has big value similar to Fig. 6. However, not all domains of surfaces have solid-like structure during full motion time. It can be seen in Fig. 13, where the time behavior of order parameter $\varphi$ and elastic stress $\sigma_{\text{el}}$ for the last domain of top surface is depicted. There are time moments when the lubricant is liquid-like ($\varphi = 0, \sigma_{\text{el}} = 0$). But the most part

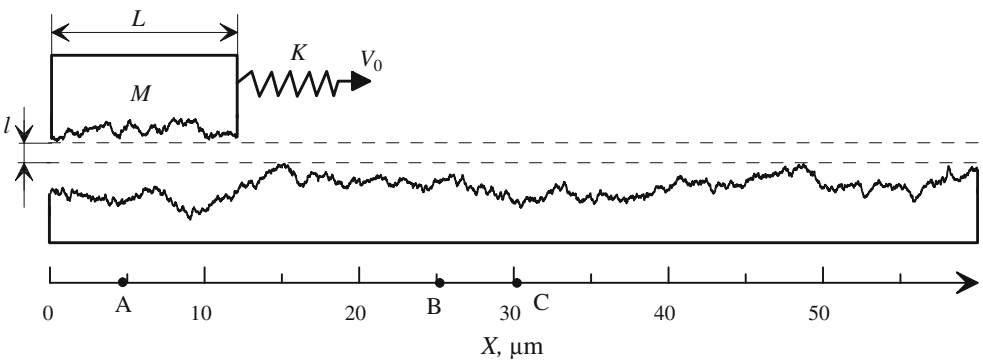


**Fig. 11** The mechanical analogue of tribological system with rough surfaces (coincide with Fig. 5), which is obtained at realization of iterative procedure given by Eq. 29 at parameters $I = 1$, $\tau_\lambda = 200$, $\Delta t = 0.25$

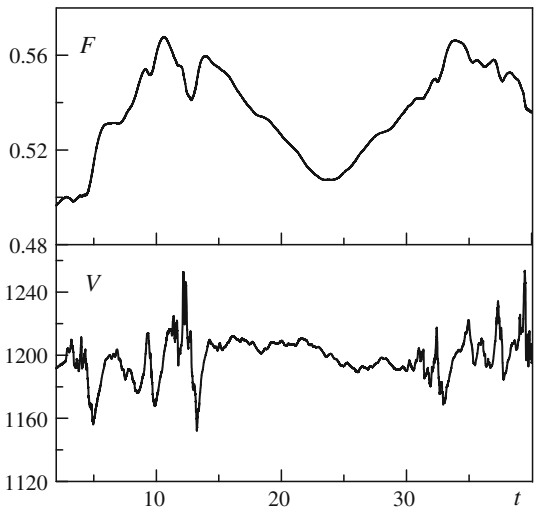


**Fig. 12** The time dependencies of friction force $F$ (mN) and shear velocity $V$ (nm/s) for parameters of Fig. 6 and $l = 1$ nm, $L = 0.12 \cdot 10^{-4}$ m, $N = 1000$, $V_0 = 1200$ nm/s, $T = 200$ K

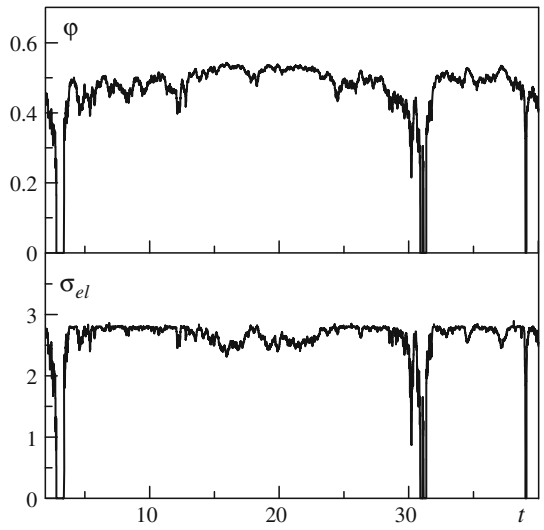


**Fig. 13** The time dependencies of order parameter $\varphi$ and elastic stress $\sigma_{el}$ for last domain of top rubbing surface at parameters of Fig. 12

of domains during friction has solid-like structure, therefore the mode of dry friction is observed. All dependencies in Figs. 12 and 13 are calculated for the time $t > 2$ s, when the stationary regime is realized.

In Fig. 14, the time dependencies of total friction force $F$ and coordinate $X$ for process of friction of rough rubbing surfaces (Fig. 11) at larger velocity $V_0$ are shown.

In accordance with this figure, the stick-slip motion mode sets in. But this regime is not strongly periodic, because the frequency of phase transitions and amplitude of friction force are not constant during time. The reason for this is the roughness of top and bottom rubbing surfaces. In the beginning of motion in time interval $t < t_A$ the system is in the dry friction mode with large value of friction force $F$. In the intervals $t_A < t < t_B$ and $t > t_C$, the stick-slip mode of motion is realized. But in the intermediate interval of time $t_B < t < t_C$ the greater number of domains has solid-like structure with non-zero shear modulus, and system as a whole has the properties of dry friction. In the bottom panel in Fig. 14 in the $X$ axis, the three points A, B, and C are shown, which correspond to the time moments $t_A$, $t_B$, and $t_C$. This points are depicted in the $X$ axis in Fig. 11. According to Fig. 14, the points A, B, and C are the coordinates of left side of top rubbing block where the transitions between different regimes of friction occur. In the study [37], taking into account the external stochastic force, the similar quasiperiodic time dependencies of stresses are obtained.

In Fig. 15, the dependence of shear velocity $V$ of top rubbing block on coordinate of this block $X$ is shown. In this figure, it is visible that during time intervals when the system is in the dry friction mode the velocity $V$ has small value. The coordinate dependence of velocity in this figure is characterized by a variable amplitude and frequency also. It is worth noting that the coordinate dependence of the shear velocity has a parabolic form. The study of dependencies of the tribological variables on the coordinate of the top rubbing block was also carried out in [38].

**Fig. 14** The time dependencies of friction force $F$ (mN) and coordinate of top rubbing block $X$ (μm) at parameters of Fig. 12 and $T = 200$ K, $V_0 = 1650$ nm/s

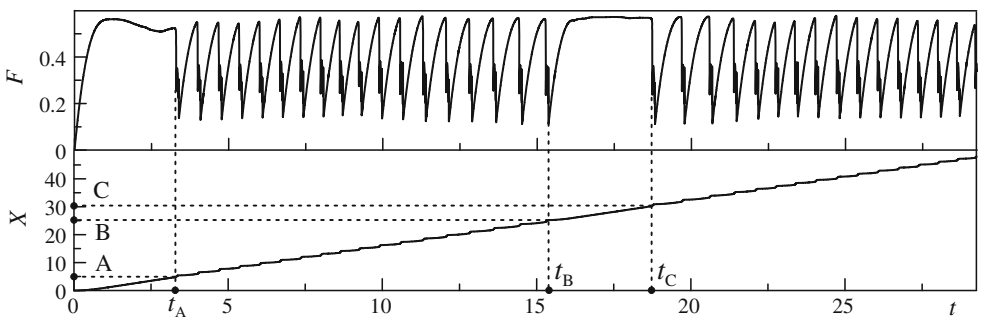

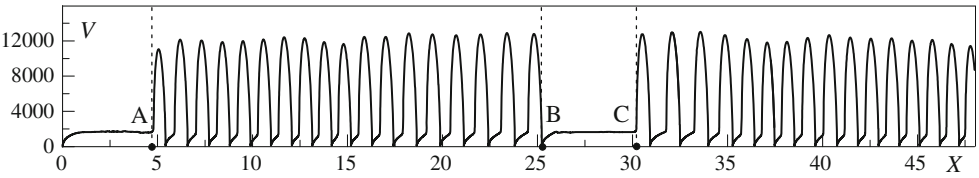


**Fig. 15** The dependence of shear velocity of top block $V$ (nm/s) on coordinate of this block $X$ (μm) at parameters of Fig. 14

## 7 Conclusions

In this study, the theoretical model based on the Landau phase transition theory is proposed in order to explain a number of effects appearing during the process of boundary friction. The dependencies of friction force on shear velocity and temperature are analyzed. At the high lubricant temperature, the shear melting is realized at smaller value of shear velocity (shear stress), and with a still higher increase in the temperature the lubricant melts even at zero shear velocity. Using the proposed theory, the mechanical analogue of tribological system has been studied, and the time dependencies of friction force are obtained for the increasing shear velocity and temperature. It is shown that in a wide range of parameters the experimentally observable stick-slip motion is realized. This stick-slip friction mode was shown as a result of the first-order phase transition between liquid-like and solid-like structures of the lubricant. When studying the effect of the temperature on melting, we have found that with the temperature increase the lubricant melts at lower relative shear velocities of the interacting surfaces. The obtained results qualitatively coincide with the experimental data. Since the model is quantitative, it may be modified to describe particular experiments.

**Acknowledgments** We express our gratitude to Bo N.J. Persson for the discussion of the study and for invitation to the Forschungszentrum Jülich (Germany) with a research visit, during which this study was carried out. We thank the organizers of conference "Joint ICTP-FANAS Conference on Trends in Nanotribology" (12-16 September 2011, Miramare, Trieste-Italy) for invitation and financial support of participation. We are grateful to Maya Sinitsa and Kyrill Zakharov for attentive reading and correction of the manuscript.

## References

1. Persson, B.N.J.: Sliding Friction. Physical Principles and Applications. Springer-Verlag, Berlin (1998)
2. Popov, V.L.: Kontaktmechanik und Reibung. Ein Lehr- und Anwendungsbuch von der Nanotribologie bis zur numerischen Simulation. Springer, Berlin (2009)
3. Yoshizawa, H., Chen, Y.-L., Israelachvili, J.: Fundamental mechanisms of interfacial friction. 1. Relation between adhesion and friction. J. Phys. Chem. **97**, 4128–4140 (1993)
4. Yoshizawa, H., Israelachvili, J.: Fundamental mechanisms of interfacial friction. 2. Stick-slip friction of spherical and chain molecules. J. Phys. Chem. **97**, 11300–11313 (1993)
5. Lyashenko, I.A.: Tribological properties of dry, fluid, and boundary friction. Tech. Phys. **56**, 701–707 (2011)
6. Popov, V.L.: Thermodynamics and kinetics of shear-induced melting of a thin layer of lubricant confined between solids. Tech. Phys. **46**, 605–615 (2001)
7. Lyashenko, I.A.: Tribological system in the boundary friction mode under a periodic external action. Tech. Phys. **56**, 869–876 (2011)
8. Khomenko, A.V., Lyashenko, I.A.: Melting of ultrathin lubricant film due to dissipative heating of friction surfaces. Tech. Phys. **52**, 1239–1243 (2007)
9. Khomenko, A.V, Lyashenko, I.A., Borisyuk, V.N.: Self-similar phase dynamics of boundary friction. Ukr. J. Phys. **54**, 1139–1148 (2009)
10. Braun, O.M., Naumovets, A.G.: Nanotribology: microscopic mechanisms of friction. Surf. Sci. Rep. **60**, 79–158 (2006)
11. Benassi, A., Vanossi, A., Santoro, G.E., Tosatti, E.: Parameter-free dissipation in simulated sliding friction. Phys. Rev. B **82**, 081401–4 (2010)
12. Khomenko, A.V., Prodanov, N.V.: Molecular dynamics of cleavage and flake formation during the interaction of a graphite surface with a rigid nanoasperity. Carbon **48**, 1234–1243 (2010)
13. Voisin, C., Renard, F., Grasso, J.-R.: Long term friction: from stick-slip to stable sliding. Geophys. Res. Lett. **34**, L13301–5 (2007)
14. Filippov, A.E., Klafter, J., Urbakh, M.: Friction through dynamical formation and rupture of molecular bonds. Phys. Rev. Lett. **92**, 135503–4 (2004)
15. Demirel, A.L., Granick, S.: Transition from static to kinetic friction in a model lubricating system. J. Chem. Phys. **109**, 6889–6897 (1998)
16. Pogrebnyak, A.D., Bratushka, S.N., Il'yashenko, M.V., Makhmudov, N.A., Kolisnichenko, O.V., Tyurin, Yu.N., Uglov, V.V., Pshik, A.V., Kaverin, M.V.: Tribological and physical-mechanical properties of protective coatings from Ni-Cr-B-Si-Fe/WC-Co-Cr before and after fission with a plasma jet. J. Frict. Wear **32**, 84–90 (2011)
17. Landau, L.D., Lifshitz, E.M.: Course of Theoretical Physics, Vol.5: Statistical Physics. Butterworth, London (1999)
18. Popov, V.L.: A theory of the transition from static to kinetic friction in boundary lubrication layers. Solid State Commun. **115**, 369–373 (2000)
19. Luengo, G., Israelachvili, J., Granick, S.: Generalized effects in confined fluids: new friction map for boundary lubrication. Wear **200**, 328–335 (1996)
20. Braun, O.M., Manini, N., Tosatti, E.: Role of lubricant molecular shape in microscopic friction. Phys. Rev. B **78**, 195402–10 (2008)
21. Aranson, I.S., Tsimring, L.S., Vinokur, V.M.: Stick-slip friction and nucleation dynamics of ultrathin liquid films. Phys. Rev. B **65**, 125402–7 (2002)
22. Khomenko, A.V., Lyashenko, I.A.: Hysteresis phenomena during melting of an ultrathin lubricant film. Phys. Solid State **49**, 936–940 (2007)
23. Lyashenko, I.A., Khomenko, A.V., Metlov, L.S.: Thermodynamics and kinetics of boundary friction. Tribol. Int. **44**, 476–482 (2011)

24. Lyashenko, I.A., Khomenko, A.V., Metlov, L.S.: Nonlinear thermodynamic model of boundary friction. J. Frict. Wear **32**, 113–123 (2011)
25. Brener, E.A., Marchenko, V.I.: Frictional shear cracks. JETP Lett. **76**, 211–214 (2002)
26. Reiter, G., Demirel, A.L., Peanasky, J., Cai, L.L., Granick, S.: Stick to slip transition and adhesion of lubricated surfaces in moving contact. J. Chem. Phys. **101**, 2606–2615 (1994)
27. Hohenberg, P.C., Halperin, B.I.: Theory of dynamic critical phenomena. Rev. Mod. Phys. **49**, 435–479 (1977)
28. Landau, L.D., Khalatnikov, I.M.: On the anomalous absorption of sound near a second-order phase transition point. Dokl. Akad. Nauk SSSR **96**, 469–472 (1954) (see also: Collected Papers of L.D. Landau, edited by D. ter Haar. Pergamon, London (1965))
29. He, G., Robbins, M.O.: Simulations of the static friction due to adsorbed molecules. Phys. Rev. B **64**, 035413–13 (2001)
30. Lyashenko, I.A.: First-order phase transition between the liquidlike and solidlike structures of a boundary lubricant. Tech. Phys. **57**, 17–26 (2012)
31. Israelachvili, J.N.: Adhesion forces between surfaces in liquids and condensable vapours. Surf. Sci. Rep. **14**, 109–159 (1992)
32. Gardiner, C.W.: Handbook of Stochastic Methods. Springer, Berlin (1983)
33. Khomenko, A.V., Lyashenko, I.A.: Phase dynamics and kinetics of thin lubricant film driven by correlated temperature fluctuations. Fluct. Noise Lett. **7**, L111–L133 (2007)
34. Press, W.H., Teukolsky, S.A., Vetterling, W.T., Flannery, B.P.: Numerical Recipes in C: The Art of Scientific Computing. Cambridge University Press, New York (1992)
35. Khomenko, A.V., Lyashenko, I.A.: Stochastic theory of ultrathin lubricant film melting in the stick-slip regime. Tech. Phys. **50**, 1408–1416 (2005)
36. Khomenko, A.V., Lyashenko, I.A., Borisyuk, V.N.: Multifractal analysis of stress time series during ultrathin lubricant film melting. Fluct. Noise Lett. **9**, 19–35 (2010)
37. Khomenko, A.V., Lyashenko, Y.A.: Periodic intermittent regime of a boundary flow. Tech. Phys. **55**, 26–32 (2010)
38. Bonelli, F., Manini, N., Cadelano, E., Colombo, L.: Atomistic simulations of the sliding friction of graphene flakes. Eur. Phys. J. B **70**, 449–460 (2009)